Chemical Vapor Deposition of Ionic Liquids for the Fabrication of Ionogel Films and Patterns

Obst, Martin; Arnauts, Giel; Cruz, Alexander John; Calderon Gonzalez, Maider; Marcoen, Kristof; Hauffman, Tom; Ameloot, Rob

Published in:
Angewandte Chemie - International Edition

DOI:
10.1002/anie.202110022

Publication date:
2021

License:
Unspecified

Document Version:
Accepted author manuscript

Chemical Vapor Deposition of Ionic Liquids for the Fabrication of Ionogel Films and Patterns

Martin Obst[a], Giel Arnauts[a], Alexander John Cruz[a,b], Maider Calderon Gonzalez[a], Kristof Marcoen[b], Tom Hauffman[b], and Rob Ameloot*[a]

[a] Dr. M. Obst, G. Arnauts, A. J. Cruz, M. Calderon Gonzalez, Prof. R. Ameloot
Centre for Membrane Separations, Adsorption, Catalysis, and Spectroscopy for Sustainable Solutions
KU Leuven
Leuven, Belgium
E-mail: rob.ameloot@kuleuven.be
[b] Dr. K. Marcoen, Prof. T. Hauffman
Research Group of Electrochemical and Surface Engineering
Vrije Universiteit Brussel
Brussels, Belgium

Abstract: Film deposition and high-resolution patterning of ionic liquids (ILs) remain a challenge, despite a broad range of applications that would benefit from this type of processing. Here, we demonstrate for the first time the chemical vapor deposition (CVD) of ILs. The IL-CVD method is based on the formation of a non-volatile IL through the reaction of two vaporized precursors. Ionogel micropatterns can be easily obtained via the combination of IL-CVD and standard photolithography, and the resulting microdrop arrays can be used as microreactors. The IL-CVD approach will facilitate leveraging the properties of ILs in a range of applications and microfabricated devices.

Due to their outstanding physical and chemical properties,[1,2] ionic liquids (ILs) are of interest for applications including chromatography,[3–6] catalysis,[3,7] batteries,[2,8–10] photovoltaics,[1,11–13] sensors,[14–18] actuators,[1,19,20] lubricants,[21–24] and wettability control.[3,25,26] Some applications, such as the integration with microelectronics, protein microarrays, and gas sensors, require the deposition and patterning of IL films.[27–31] Direct spray-coating is hindered by the high viscosity of ILs. The use of solvents as dilutants is often undesired and may result in non-uniformity (e.g., because of droplet formation during drying) and an uncontrolled thickness. A vapor phase deposition method would be desirable to overcome these challenges. Physical vapor deposition (PVD), through direct IL evaporation and condensation on a surface, has been demonstrated for alkylimidazolium bis(trifluoromethylsulfonyl)imides (Tf_2N).[32–34] However, PVD of ILs requires an ultra-high vacuum (< 10^{-8} mbar) due to their low vapor pressure (< 10^{-3} mbar at moderate temperatures), resulting in low deposition rates only suited for fundamental studies.[32–35] In specific cases, the surface-catalyzed cleavage of an ester-functionalized IL with a higher vapor pressure can be exploited to obtain a carboxylate-anchored IL monolayer on the surface.[36] The formation of patterned IL films is typically achieved by printing techniques, including direct,[27] indirect,[27,37] and inkjet printing.[38,39] However, these wet techniques have a limited resolution, which is controlled by the viscosity of the IL, the stamp geometry, or the minimum ejected volume, and have a limited throughput since patterns on larger areas are deposited sequentially.[38] High-resolution ionogel patterns have been fabricated by lithography and the use of photoresist-IL mixtures.[40] However, the scope of this approach is limited since only for one IL, 1-butyl-3-methylimidazolium dicyanamide, the mixtures were long-term stable and retained their transparency, regardless of the photoresist tested.

In chemical vapor deposition (CVD), a thin film of the desired compound is formed on the substrate through the reaction of volatile precursors, typically enabling excellent thickness control.[41] CVD is a cornerstone technology in surface engineering and microdevice fabrication.[41,42] Although CVD is mostly associated with inorganic materials,[43] deposition processes have been demonstrated for organic and hybrid polymers,[42] metal-organic frameworks (MOFs),[44–46] and graphene.[47,48] The observation that many ILs can be synthesized from precursors with a significant vapor pressure inspired us to explore the novel concept of “IL-CVD”: reacting two precursor vapors to form a non-volatile IL on the surface. IL formation from precursor vapors occurs in the chemical distillation of ILs. For instance, alkylimidazolium ILs can be thermally decomposed to their neutral precursors (imidazoles and alkyl halides), which evaporate and react back to the original IL upon condensation.[49–51] This concept has also been demonstrated for carbamate,[52] silylimidazolium,[53] and protic ILs.[54] In contrast to chemical distillation, IL-CVD allows for the formation of well-defined IL thin films. Moreover, as IL-CVD would be compatible with a standard lithography workflow, we investigated its potential in IL patterning.

The IL 1-butyl-3-methylimidazolium bromide ([bmim]Br) is formed by a quaternization reaction of 1-methylimidazole (mim) and 1-bromobutane (BB),[55] typically at elevated temperatures under solvent-free conditions.[56,57] As a first step towards a CVD method, liquid mim was exposed to vapors of the more volatile precursor BB at 80 °C. As a result of BB absorption into the liquid nucleophile precursor, mim could be successfully transformed into [bmim]Br in high purity and 82 % yield based on mim (Figure 1a). By following the same protocol, the scope of this vapor quaternization approach could be extended to other imidazoles, aliphatic amines, and pyridine as nucleophile precursors (Table S1). Unreacted precursors remaining in the IL are easily removed by heating in dynamic vacuum due to the non-volatility of the IL. ^{1}H NMR proves complete removal of mim (initially 16 mol%) from a mim/[bmim]Br mixture by heating to 120 °C in dynamic vacuum (Figure 1b). Alternatively, excess mim in the formed IL can be fully reacted to [bmim]Br by a longer BB exposure. In addition, the IL

quantity can be increased by absorbing more mim from the vapor phase into the formed [bmim]Br, leading to an equilibrium mixture of 68 mol% mim (at 120°C), and subsequent exposure to BB leading to full conversion (Figure 1b).

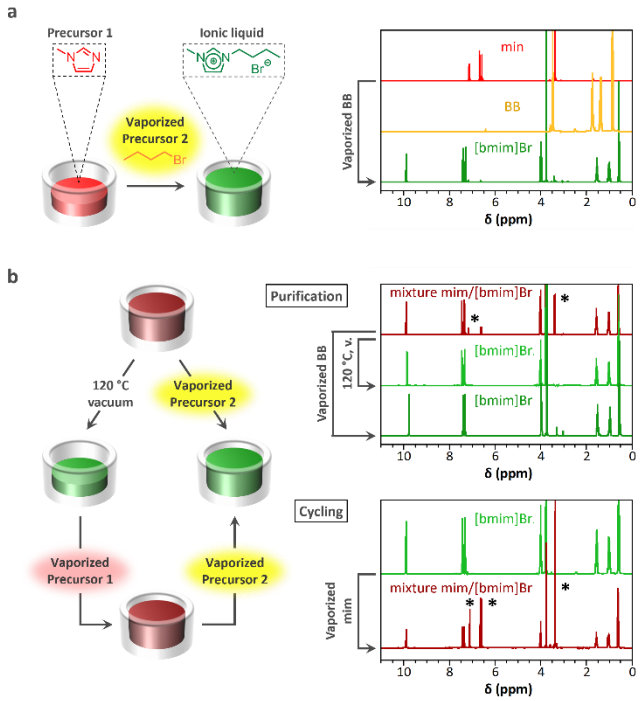

Figure 1. Bulk [bmim]Br formation from precursor vapors. a, IL formation via BB vapor absorbing into liquid mim (80 °C, 24 h). ^{1}H NMR spectra ($CDCl_3$) of mim, BB, and formed [bmim]Br (97 % purity). **b**, IL purification and cycling (dark red = mim/[bmim]Br mixture) and ^{1}H NMR spectra ($CDCl_3$) recorded before and after purification and cycling experiments, with a mim/[bmim]Br mixture containing 16 mol% mim before purification (top) and 68 mol% mim after mim vapor absorption for cycling (bottom); mim peaks are indicated with an asterisk.

Next, the IL formation from precursor vapors was extended to film deposition. To form IL on a silicon wafer, a thin film of a polymer photoresist with affinity for the nucleophile mim was deposited first. Whereas mim would rapidly desorb from the bare substrate once dosing of the vapor is halted, a suitable resist layer in which mim infiltrates can act as a buffer reservoir. Polar polymers such as Novolak resists, polyvinylpyrrolidone, and polyimides proved suitable for this purpose, as confirmed by absorption tests and their position within the mim Hansen sphere (Figures S4-7). In a second step, BB vapor is introduced, which infiltrates into the resist and reacts with mim to form an 'ionogel' (Figure 2a). Organic ionogels obtained by IL immobilization in a polymer matrix[58–61] have a broad spectrum of applications, e.g., in actuators,[20,62,63] sensors,[40,64,65] capacitors,[66,67] and transistors.[68,69] Figure 2b shows the IL-CVD flow reactor in which the precursor vapors are sequentially introduced by a nitrogen carrier stream. To gain insight into the timescale of IL generation in a 3 µm resist film, the absorption of mim and formation of [bmim]Br in the resist was monitored by *in situ* FTIR spectroscopy. Figure 2c shows the ring vibration[70,71] absorbance of mim (1518 cm^{-1}) and [bmim]Br (1167 cm^{-1}) over time. In the first step, the mim band increases until stabilization after 10 h. Next, BB is introduced, resulting in the rise of the [bmim]Br band and a simultaneous decrease of the mim band, which approaches zero while the [bmim]Br band stabilizes. The FTIR spectra of the ionogel after heating to remove unreacted precursors demonstrate the successful formation of [bmim]Br (Figure 2d). The ionogel film was analyzed by thermogravimetric analysis coupled with mass spectrometry (TG-MS). A temperature profile with isothermal plateaus at 300 and 800 °C was used to separate the thermal decomposition of [bmim]Br and the resist, and to determine the IL contents of the ionogel (Figure S9). Dequaternization of [bmim]Br, to again form volatile alkylimidazoles and alkylbromides, occurs around 250-300 °C (Figure 2e). Upon increasing the temperature to 800 °C, the resist decomposes, illustrated by the detection of benzene and cresole fragments (Figure S10). Infiltrating mim for 24 h into the resist layer, followed by BB infiltration for 48 h, resulted in an ionogel with 34 wt% [bmim]Br (Figure 2f). Repeating the infiltration-reaction sequence on the same film increased the IL content to 44 wt%, and four cycles yielded 56 wt%. Ionogels with a comparable IL content have been used as actuators[62,72] and capacitors.[66] Shortening the mim evaporation time to 4 h results in 7 wt% only, even after the second cycle. Apparently, the infiltration rate of mim into the resist is limited by slow diffusion, and the switch to BB leads to considerable mim desorption from the surface and upper part of the film. Still, when the infiltration time is sufficiently long, a homogeneous distribution of [bmim]Br within the ionogel is obtained, as indicated by time-of-flight secondary ion mass spectrometry (ToF-SIMS) depth profiling: constant signals of IL fragments are detected upon sputtering until reaching the wafer surface (Figure 2g). The ionogel possesses a thickness of about 5 µm (Figure S11).

Ionogel micropatterns can be easily obtained via the combination of IL-CVD and standard photolithography since the precursors selectively absorb into the photoresist and not onto the bare substrate. As an illustration, well-defined microdrop patterns were formed when subjecting a resist pattern on a Teflon-coated wafer to IL-CVD. During the CVD process, precursor infiltration and IL formation liquefy the solid resist, resulting in an in-plane contraction and the formation of an ionogel microdrop array due to the high contact angle of the substrate (Figure 3a). For instance, a 100 µm square pattern in a 3 µm thick resist layer was converted into an array of ionogel microdrops with a diameter of 85 µm and a height of 20 µm (Figures 3b,c and S12, S15). Ionogel microdrops were also formed starting from 10 µm resist patterns (Figure S13). The use of other surfaces instead of Teflon (silicon Si-OH and Si-H terminated, HDMS coating) resulted in coalescence or irregular ionogel structures (Figure S14).

Because of their non-volatility and solvent properties, ILs have been used as crystallization media for KBr,[73] pentacene,[74] and a variety of pharmaceuticals.[75] Ionogel micropatterns enable to exploit this crystallization mechanism in an area-selective fashion. This approach opens up an entirely novel route for the integration of molecular crystalline compounds into microfabrication, as demonstrated here for methyl-4-hydroxybenzoate (MHB), a compound with non-linear optical properties.[76] When MHB is sublimed at 120 °C in a closed vial containing the ionogel pattern, the vapor absorbs into the ionogel microdrops and MHB crystallizes upon cooling to room temperature. Since no MBH adsorbs on the substrate surface, crystallization occurs exclusively from the ionogel, resulting in well-defined crystal-covered areas with a height and width of 60 and 150 µm, respectively, both several times larger than the dimensions of the initial ionogel microdrops (Figure 4). In addition, thanks to their monomer absorption properties, ILs enable polymerization from the vapor phase, as demonstrated for polyurea[77] and poly(2-hydroxyethyl methacrylate).[78] Similarly, ionogel microdrops can act as microreactors for the polymerization of 3,4-ethylenedioxythiophene (EDOT).[79] By first absorbing EDOT at 120 °C and subsequently introducing I_2 vapor at 50 °C as an oxidant, PEDOT-coated microdrops are obtained with a similar shape as the ionogel and a minor increase in height (Figure 4). The presence of PEDOT was confirmed by FTIR spectroscopy (Figure S8).

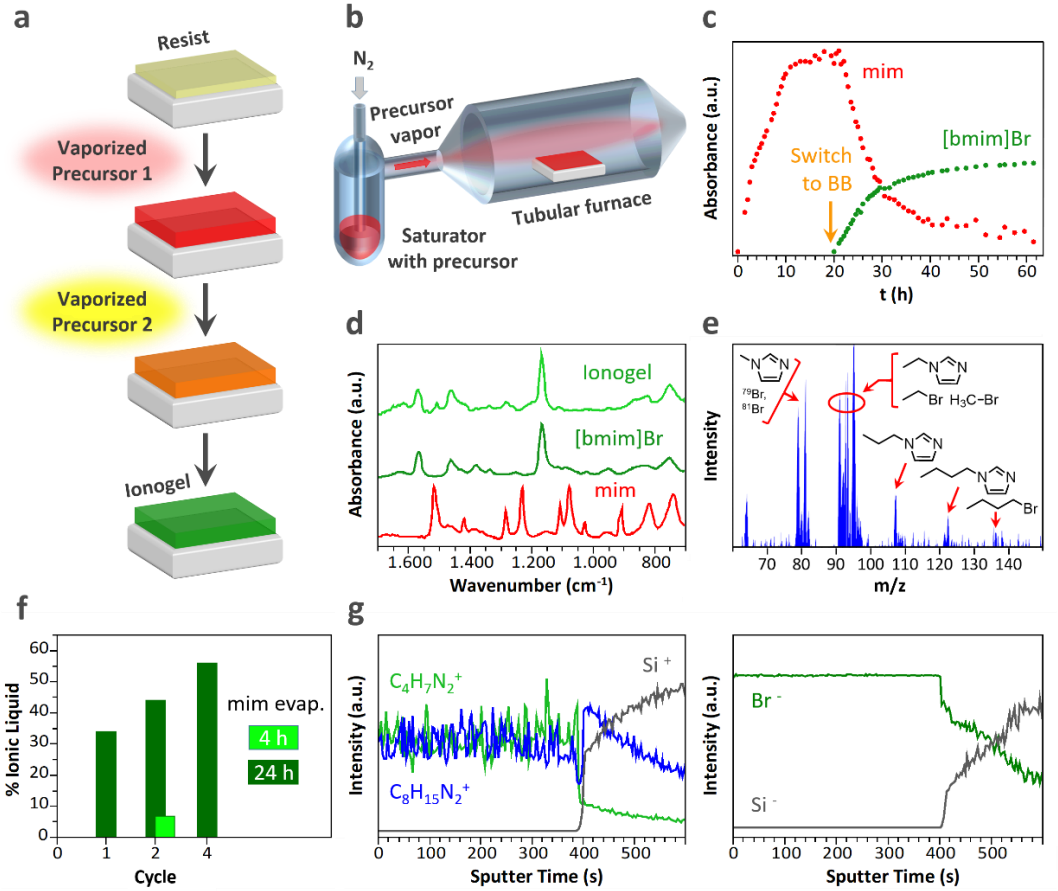

Figure 2. [bmim]Br film formation from precursor vapors. a, IL film deposition sequence from vapor phase precursors. **b**, Reaction chamber setup applied for IL-CVD. **c**, FTIR monitoring of mim absorption and [bmim]Br formation in resist. **d**, FTIR spectra of an ionogel consisting of [bmim]Br and resist (top) and bulk [bmim]Br (middle) and mim (bottom) for comparison. **e**, Mass spectra obtained by TG-MS from the ionogel at 300°C. **f**, [bmim]Br contents in the ionogel (wt%) as a function of cycle number. **g**, ToF-SIMS depth profiles of an ionogel with a [bmim]Br content of 34 wt%. Both the positive scan (left) and the negative scan (right) indicate the homogeneous distribution of the IL in the film.

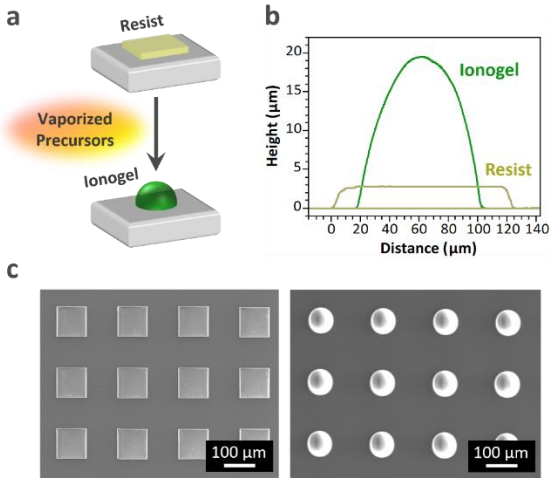

Figure 3. Formation of ionogel micropatterns by IL-CVD. a, Schematic representation of ionogel microdrop formation. **b**, Height profiles of the photoresist square pattern and ionogel microdrops. **c**, SEM images of the photoresist pattern before (left) and after conversion to ionogel microdrops by IL-CVD (right).

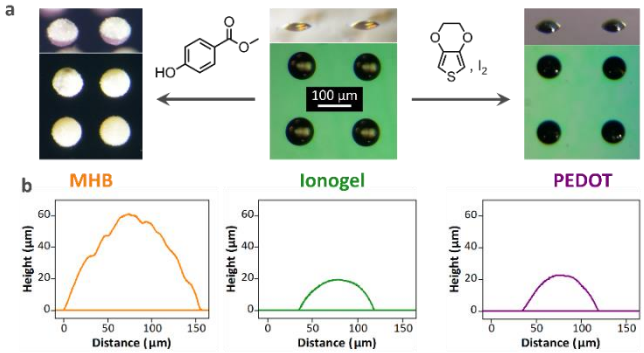

Figure 4. Application of ionogel microdrops. a, Optical microscopy images: Crystallization of MBH (left, white microdrops) and coating with PEDOT (right, black microdrops). **b**, Height profiles of ionogel microdrops (middle), after crystallization of MBH (left), and after coating with PEDOT (right).

For the first time, we demonstrated the CVD of an IL. The strength of the IL-CVD method to deposit ionogel microstructures and the ability of the vaporized precursors to conformally coat three-dimensional substrates will facilitate leveraging the properties of ILs in a range of devices and applications including microsupercapacitors and microbatteries,[80–83] solar cells,[11,12] actuators,[19] sensors,[15,16,29,30] membrane separation processes,[84] and display textiles.[85]

Acknowledgements

We acknowledge funding from the European Union in the Horizon 2020 FETOPEN-1-2016-2017 research and innovation program (grant agreement 801464) and from the Research Foundation Flanders (FWO Vlaanderen) in research and infrastructure projects G0E6319N and I014018N.

Keywords: Ionic liquid • ionogel • chemical vapor deposition • micropattern • photolitography

[1] D. R. MacFarlane, N. Tachikawa, M. Forsyth, J. M. Pringle, P. C. Howlett, G. D. Elliott, J. H. Davis, M. Watanabe, P. Simon, C. A. Angell, *Energy Environ. Sci.* **2014**, *7*, 232–250.
[2] M. Watanabe, M. L. Thomas, S. Zhang, K. Ueno, T. Yasuda, K. Dokko, *Chemical Reviews* **2017**, *117*, 7190–7239.
[3] B. Xin, J. Hao, *Chem. Soc. Rev.* **2014**, *43*, 7171–7187.
[4] H. Qiu, A. K. Mallik, M. Takafuji, S. Jiang, H. Ihara, *The Analyst* **2012**, *137*, 2553.
[5] X. Sun, Y. Zhu, P. Wang, J. Li, C. Wu, J. Xing, *Journal of Chromatography A* **2011**, *1218*, 833–841.
[6] K. Huang, X. Zhang, D. W. Armstrong, *Journal of Chromatography A* **2010**, *1217*, 5261–5273.
[7] R. Skoda-Földes, *Molecules* **2014**, *19*, 8840–8884.
[8] T. Yim, M.-S. Kwon, J. Mun, K. T. Lee, *Israel Journal of Chemistry* **2015**, *55*, 586–598.
[9] H. Srour, L. Chancelier, E. Bolimowska, T. Gutel, S. Mailley, H. Rouault, C. C. Santini, *Journal of Applied Electrochemistry* **2016**, *46*, 149–155.
[10] J. S. Moreno, Y. Deguchi, S. Panero, B. Scrosati, H. Ohno, E. Simonetti, G. B. Appetecchi, *Electrochimica Acta* **2016**, *191*, 624–630.
[11] K. Fredin, M. Gorlov, H. Pettersson, A. Hagfeldt, L. Kloo, G. Boschloo, *The Journal of Physical Chemistry C* **2007**, *111*, 13261–13266.
[12] S. Ito, K. Takahashi, *International Journal of Photoenergy* **2012**, *2012*, 1–6.
[13] D. Högberg, B. Soberats, S. Uchida, M. Yoshio, L. Kloo, H. Segawa, T. Kato, *Chemistry of Materials* **2014**, *26*, 6496–6502.
[14] A. Abo-Hamad, M. A. AlSaadi, M. Hayyan, I. Juneidi, M. A. Hashim, *Electrochimica Acta* **2016**, *193*, 321–343.
[15] V. V. Singh, A. K. Nigam, A. Batra, M. Boopathi, B. Singh, R. Vijayaraghavan, *International Journal of Electrochemistry* **2012**, *2012*, 1–19.
[16] M. J. A. Shiddiky, A. A. J. Torriero, *Biosensors and Bioelectronics* **2011**, *26*, 1775–1787.
[17] A. Rehman, X. Zeng, *RSC Advances* **2015**, *5*, 58371–58392.
[18] S. V. Muginova, D. A. Myasnikova, S. G. Kazarian, T. N. Shekhovtsova, *Analytical Sciences* **2017**, *33*, 261–274.
[19] S. Imaizumi, Y. Kato, H. Kokubo, M. Watanabe, *The Journal of Physical Chemistry B* **2012**, *116*, 5080–5089.
[20] C. Keplinger, J.-Y. Sun, C. C. Foo, P. Rothemund, G. M. Whitesides, Z. Suo, *Science* **2013**, *341*, 984–987.
[21] M.-D. Avilés, R. Pamies, J. Sanes, F.-J. Carrión, M.-D. Bermúdez, *Coatings* **2019**, *9*, 710.
[22] Y. Ma, Z. Li, H. Wang, H. Li, *Journal of Colloid and Interface Science* **2019**, *534*, 469–479.
[23] J. Pu, D. Huang, L. Wang, Q. Xue, *Colloids and Surfaces A: Physicochemical and Engineering Aspects* **2010**, *372*, 155–164.
[24] J. Liu, J. Li, B. Yu, B. Ma, Y. Zhu, X. Song, X. Cao, W. Yang, F. Zhou, *Langmuir* **2011**, *27*, 11324–11331.
[25] B. S. Lee, Y. S. Chi, J. K. Lee, I. S. Choi, C. E. Song, S. K. Namgoong, S. Lee, *Journal of the American Chemical Society* **2004**, *126*, 480–481.
[26] Y. S. Chi, J. K. Lee, S. Lee, I. S. Choi, *Langmuir* **2004**, *20*, 3024–3027.
[27] C. A. Gunawan, M. Ge, C. Zhao, *Nat Commun* **2014**, *5*, 3744.
[28] M. Ge, R. Gondosiswanto, C. Zhao, *Inorganic Chemistry Communications* **2019**, *107*, 107458.
[29] G. Hussain, M. Ge, C. Zhao, D. S. Silvester, *Analytica Chimica Acta* **2019**, *1072*, 35–45.
[30] M. Ge, G. Hussain, D. B. Hibbert, D. S. Silvester, C. Zhao, *Electroanalysis* **2019**, *31*, 66–74.
[31] P. D. Haller, R. J. Frank-Finney, M. Gupta, *Macromolecules* **2011**, *44*, 2653–2659.
[32] T. Cremer, M. Killian, J. M. Gottfried, N. Paape, P. Wasserscheid, F. Maier, H.-P. Steinrück, *ChemPhysChem* **2008**, *9*, 2185–2190.
[33] J. C. S. Costa, A. Mendes, L. M. N. B. F. Santos, *ChemPhysChem* **2016**, *17*, 2123–2127.
[34] J. C. S. Costa, A. F. S. M. G. Coelho, A. Mendes, L. M. N. B. F. Santos, *Applied Surface Science* **2018**, *428*, 242–249.
[35] T. Cremer, M. Stark, A. Deyko, H.-P. Steinrück, F. Maier, *Langmuir* **2011**, *27*, 3662–3671.
[36] T. Xu, T. Waehler, J. Vecchietti, A. Bonivardi, T. Bauer, J. Schwegler, P. S. Schulz, P. Wasserscheid, J. Libuda, *Angew. Chem. Int. Ed.* **2017**, *56*, 9072–9076.
[37] X. Zhang, Y. Cai, *Beilstein Journal of Nanotechnology* **2012**, *3*, 33–39.
[38] V. J. Cadarso, J. Perera-Nuñez, A. Mendez-Vilas, L. Labajos-Broncano, M.-L. González-Martín, J. Brugger, *Journal of Materials Research* **2014**, *29*, 2100–2107.
[39] S. G. Hashmi, M. Ozkan, J. Halme, K. D. Misic, S. M. Zakeeruddin, J. Paltakari, M. Grätzel, P. D. Lund, *Nano Energy* **2015**, *17*, 206–215.
[40] N. A. Bakhtina, U. Loeffelmann, N. MacKinnon, J. G. Korvink, *Adv. Funct. Mater.* **2015**, *25*, 1683–1693.
[41] L. Sun, G. Yuan, L. Gao, J. Yang, M. Chhowalla, M. H. Gharahcheshmeh, K. K. Gleason, Y. S. Choi, B. H. Hong, Z. Liu, *Nat Rev Methods Primers* **2021**, *1*, 5.
[42] A. M. Coclite, R. M. Howden, D. C. Borrelli, C. D. Petruczok, R. Yang, J. L. Yagüe, A. Ugur, N. Chen, S. Lee, W. J. Jo, A. Liu, X. Wang, K. K. Gleason, *Advanced Materials* **2013**, *25*, 5392–5423.
[43] R. W. Johnson, A. Hultqvist, S. F. Bent, *Materials Today* **2014**, *17*, 236–246.
[44] I. Stassen, M. Styles, G. Grenci, H. V. Gorp, W. Vanderlinden, S. D. Feyter, P. Falcaro, D. D. Vos, P. Vereecken, R. Ameloot, *Nature Materials* **2016**, *15*, 304–310.
[45] A. J. Cruz, I. Stassen, M. Krishtab, K. Marcoen, T. Stassin, S. Rodríguez-Hermida, J. Teyssandier, S. Pletincx, R. Verbeke, V. Rubio-Giménez, S. Tatay, C. Martí-Gastaldo, J. Meersschaut, P. M. Vereecken, S. De Feyter, T. Hauffman, R. Ameloot, *Chemistry of Materials* **2019**, *31*, 9462–9471.
[46] I. Stassen, D. De Vos, R. Ameloot, *Chemistry - A European Journal* **2016**, *22*, 14452–14460.
[47] L. Cai, G. Yu, *Small Methods* **2019**, 1900071.
[48] O. Simionescu, R. C. Popa, A. Avram, G. Dinescu, *Plasma Processes and Polymers* **2020**, DOI 10.1002/ppap.201900246.
[49] Z.-J. Chen, H.-W. Xi, K. H. Lim, J.-M. Lee, *Angewandte Chemie International Edition* **2013**, *52*, 13392–13396.
[50] G. Li, Z. Xue, B. Cao, C. Yan, T. Mu, *ACS Sustainable Chemistry & Engineering* **2016**, *4*, 6258–6262.
[51] J. Zhou, H. Sui, Z. Jia, Z. Yang, L. He, X. Li, *RSC Advances* **2018**, *8*, 32832–32864.
[52] C. P. Song, Q. Y. Yap, M. Y. aigness Chong, R. Ramakrishnan Nagasundara, R. Vijayaraghavan, D. R.

MacFarlane, E.-S. Chan, C.-W. Ooi, *ACS Sustainable Chem. Eng.* **2018**, *6*, 10344–10354.
[53] M. Köckerling, T. Peppel, P. Thiele, S. P. Verevkin, V. N. Emel'yanenko, A. A. Samarov, W. Ruth, *Eur. J. Inorg. Chem.* **2015**, *2015*, 4032–4037.
[54] A. W. T. King, J. Asikkala, I. Mutikainen, P. Järvi, I. Kilpeläinen, *Angew. Chem. Int. Ed.* **2011**, *50*, 6301–6305.
[55] J. C. Schleicher, A. M. Scurto, *Green Chem.* **2009**, *11*, 694.
[56] A. Kamal, G. Chouhan, *Advanced Synthesis & Catalysis* **2004**, *346*, 579–582.
[57] E. R. Parnham, R. E. Morris, *Chem. Mater.* **2006**, *18*, 4882–4887.
[58] E. Andrzejewska, A. Marcinkowska, A. Zgrzeba, *Polimery* **2017**, *62*, 344–352.
[59] J. Le Bideau, L. Viau, A. Vioux, *Chem. Soc. Rev.* **2011**, *40*, 907–925.
[60] T. P. Lodge, *Science* **2008**, *321*, 50–51.
[61] R. Sahrash, A. Siddiqa, H. Razzaq, T. Iqbal, S. Qaisar, *Heliyon* **2018**, *4*, e00847.
[62] Y. Liu, C. Lu, S. Twigg, M. Ghaffari, J. Lin, N. Winograd, Q. M. Zhang, *Sci Rep* **2013**, *3*, 973.
[63] B. Chen, J. J. Lu, C. H. Yang, J. H. Yang, J. Zhou, Y. M. Chen, Z. Suo, *ACS Appl. Mater. Interfaces* **2014**, *6*, 7840–7845.
[64] M. D. Bennett, D. J. Leo, *Sensors and Actuators A: Physical* **2004**, *115*, 79–90.
[65] J. Sun, Y. Yuan, G. Lu, L. Li, X. Zhu, J. Nie, *J. Mater. Chem. C* **2019**, *7*, 11244–11250.
[66] M. Cowell, R. Winslow, Q. Zhang, J. Ju, J. Evans, P. Wright, *J. Phys.: Conf. Ser.* **2014**, *557*, 012061.
[67] A. F. Visentin, M. J. Panzer, *ACS Appl. Mater. Interfaces* **2012**, *4*, 2836–2839.
[68] K. H. Lee, M. S. Kang, S. Zhang, Y. Gu, T. P. Lodge, C. D. Frisbie, *Adv. Mater.* **2012**, *24*, 4457–4462.
[69] J. Lee, M. J. Panzer, Y. He, T. P. Lodge, C. D. Frisbie, *J. Am. Chem. Soc.* **2007**, *129*, 4532–4533.
[70] V. H. Paschoal, L. F. O. Faria, M. C. C. Ribeiro, *Chem. Rev.* **2017**, *117*, 7053–7112.
[71] R. Ramasamy, **2015**, *8*, 5.
[72] J. Ding, D. Zhou, G. Spinks, G. Wallace, S. Forsyth, M. Forsyth, D. MacFarlane, *Chem. Mater.* **2003**, *15*, 2392–2398.
[73] S. Kato, Y. Takeyama, S. Maruyama, Y. Matsumoto, *Crystal Growth & Design* **2010**, *10*, 3608–3611.
[74] Y. Takeyama, S. Maruyama, Y. Matsumoto, *Crystal Growth & Design* **2011**, *11*, 2273–2278.
[75] C. C. Weber, S. A. Kulkarni, A. J. Kunov-Kruse, R. D. Rogers, A. S. Myerson, *Crystal Growth & Design* **2015**, *15*, 4946–4951.
[76] W. Hou, R. I. Ristic, K. Srinivasan, R. M. Vrcelj, R. B. Hammond, D. B. Sheen, J. N. Sherwood, *Cryst. Growth Des.* **2019**, 11.
[77] Y. Ohsawa, R. Takahashi, S. Maruyama, Y. Matsumoto, *ACS Macro Letters* **2016**, 5.
[78] R. J. Frank-Finney, L. C. Bradley, M. Gupta, *Macromolecules* **2013**, *46*, 6852–6857.
[79] B. Le Ouay, M. Boudot, T. Kitao, T. Yanagida, S. Kitagawa, T. Uemura, *J. Am. Chem. Soc.* **2016**, *138*, 10088–10091.
[80] N. A. Kyerematen, T. Brousse, D. Pech, *Nature Nanotech* **2017**, *12*, 7–15.
[81] F. Bu, W. Zhou, Y. Xu, Y. Du, C. Guan, W. Huang, *npj Flex Electron* **2020**, *4*, 31.
[82] B. Qiu, B. Lin, F. Yan, *Polym. Int.* **2013**, *62*, 335–337.
[83] C. Lian, H. Liu, J. Wu, *J. Phys. Chem. C* **2018**, *122*, 18304–18310.
[84] X. Yan, S. Anguille, M. Bendahan, P. Moulin, *Separation and Purification Technology* **2019**, *222*, 230–253.
[85] X. Shi, Y. Zuo, P. Zhai, J. Shen, Y. Yang, Z. Gao, M. Liao, J. Wu, J. Wang, X. Xu, Q. Tong, B. Zhang, B. Wang, X. Sun, L. Zhang, Q. Pei, D. Jin, P. Chen, H. Peng, *Nature* **2021**, *591*, 240–245.